






Research Article

Toward the Optimization of (+)-[¹¹C]PHNO Synthesis: Time Reduction and Process Validation

Sarah Pfaff,¹ Cécile Philippe ¹, Lukas Nics ¹, Neydher Berroterán-Infante ¹, Katharina Pallitsch,² Christina Rami-Mark,¹ Ana Weidenauer,³ Ulrich Sauerzopf,³ Matthäus Willeit,³ Markus Mitterhauser ^{1,4}, Marcus Hacker,¹ Wolfgang Wadsak ^{1,5}, and Verena Pichler¹

¹Department of Biomedical Imaging and Image-guided Therapy, Division of Nuclear Medicine, Medical University of Vienna, Vienna, Austria

²Institute of Organic Chemistry, University of Vienna, Vienna, Austria

³Department of Psychiatry and Psychotherapy, Division of General Psychiatry, Medical University of Vienna, Vienna, Austria

⁴Ludwig-Boltzmann-Institute Applied Diagnostics, Vienna, Austria

⁵CBmed GmbH-Center for Biomarker Research in Medicine, Graz, Austria

Correspondence should be addressed to Lukas Nics; lukas.nics@meduniwien.ac.at

Received 20 January 2019; Revised 19 July 2019; Accepted 30 August 2019; Published 30 September 2019

Academic Editor: Ralf Schirmmacher

Copyright © 2019 Sarah Pfaff et al. This is an open access article distributed under the Creative Commons Attribution License, which permits unrestricted use, distribution, and reproduction in any medium, provided the original work is properly cited.

(+)-[¹¹C]PHNO, a dopamine D_{2/3} receptor agonistic radiotracer, is applied for investigating the dopaminergic system via positron emission tomography (PET). An improved understanding of neuropsychiatric disorders associated with dysfunctions in the dopamine system and the underlying mechanism is a necessity in order to promote the development of new potential therapeutic drugs. In contrast to other broadly applied ¹¹C-radiopharmaceuticals, the production of this radiotracer requires a challenging four-step radiosynthesis involving harsh reaction conditions and reactants as well as an inert atmosphere. Consequently, the production is prone to errors and troubleshooting after failed radiosyntheses remains time consuming. Hence, we aimed to optimize the radiosynthesis of (+)-[¹¹C]PHNO for achieving better activity yields without loss of product quality. Therefore, we synthesized (+)-[¹¹C]PHNO and omitted all heating and cooling steps leading to higher activity yields. As a result, radiosynthesis fully conducted at room temperature led to a time-reduced production procedure that saves about 5 min, which is an appreciable decay-prevention of around 15% of the activity yield. Additionally, we established a troubleshooting protocol by investigating reaction intermediates, byproducts, and impurities. Indeed, partial runs enabled the assignment of byproducts to their associated error source. Finally, we were able to generate a decision tree facilitating error detection in (+)-[¹¹C]PHNO radiosynthesis.

1. Introduction

The dopamine system is a key player in many neuropsychiatric disorders like schizophrenia, Parkinson's disease, or attention-deficit hyperactivity disorder [1–3]. (+)-PHNO ((+)-4-propyl-3,4,4a,5,6,10b-hexahydro-2H-naphtho[1,2-b][1,4]oxazin-9-ol hydrochloride) is a well-described agonist for the dopamine D_{2/3} receptor subtypes [4–6]. This compound binds to dopamine D₂ receptors in their high affinity

state and has high affinity for the dopamine D₃ receptor subtype, making it a virtual D₃ selective probe in the ventrobasal striatum and brainstem dopaminergic nuclei [4]. It is one of the most important imaging agents measuring changes of extracellular dopamine, as it can be easily displaced by endogenous dopamine in so-called competition experiments, where dopamine-releasing agents such as amphetamine are administered [6, 7]. (+)-[¹¹C]PHNO shows high potential to bring new insights into poorly

understood physiological processes of a variety of neuropsychiatric disorders. Recently, the application of this tracer in healthy subjects and patients suffering from schizophrenia showed an enhanced dopamine release in patients with schizophrenia [8, 9]. The synthesis of ^{11}C -radiopharmaceuticals is highly challenging due to the relatively short half-life of carbon-11 (20.4 min). Consequently, a prerequisite for achieving a reasonable activity yield is a reliable production within two to three half-lives [10]. Furthermore, a fundamental requirement for this particular radiotracer is high molar activity as pharmacological doses cause side effects, like nausea [11]. (+)- ^{11}C]PHNO radiosynthesis has been published by several working groups describing synthetic routes via carbon-11 radiolabeling either on the 1-position or the 3-position of the propyl moiety (Figure 1) [12–14]. To the best of our knowledge, $[3\text{-}^{11}\text{C}]\text{-}(+)\text{-PHNO}$ radiosynthesis has not become widespread, whereas $[1\text{-}^{11}\text{C}]\text{-}(+)\text{-PHNO}$ is widely applied in clinical studies [15–17]. Radiolabeling of the common (+)- $[1\text{-}^{11}\text{C}]\text{PHNO}$ (further stated as (+)- ^{11}C]PHNO to be in accordance with the literature) starts with generation of ^{11}C]propionic acid chloride, which can be obtained by a Grignard reaction from ^{11}C]CO₂ and ethylmagnesium bromide and subsequent conversion with thionyl chloride (SOCl₂) (Figure 1, compounds 1 and 2) [18–20]. This highly reactive acyl chloride readily reacts with the precursor ((+)-HNO) to give an intermediate amide (Figure 1, compound 3). Finally, the amide is reduced and the product is purified by semipreparative high-performance liquid chromatography (HPLC). However, this radiolabeling procedure is very demanding as inert conditions and extremely harsh reagents are required. Therefore, the automated synthesis needs high technical effort. As an alternative to the conventional vessel-based approach, our working group reported an in-loop method for (+)- ^{11}C]PHNO synthesis. This method facilitates the establishment of (+)- ^{11}C]PHNO in other PET facilities [21].

Although this method improved the production of (+)- ^{11}C]PHNO, the susceptibility to humidity as well as oxygen contamination remains an unsolved problem. As a consequence, (+)- ^{11}C]PHNO synthesis has the highest failure rate within our facility. After a failed production run, an extensive validation process starts for investigating which of the numerous steps led to the radiosynthetic failure. During troubleshooting, the impact of the reaction temperature needs special considerations. Wilson et al. reported that the reaction temperature regulated the formation of byproducts: the reduction of the carboxyl-group at temperatures below -30°C results in a lower number of side products compared to higher temperatures [12].

Therefore, the major goal of this study was to reduce the duration of the radiosynthesis by shortening heating and cooling times and to validate the impact of these omitted temperature regulating procedures. In the end, the radiosynthetic procedure may be possible completely at room temperature. Furthermore, we aimed to evaluate each reaction step in order to understand the influence of the individual reagents on the production process. Obviously, the introduction of moisture is the most common problem, but

investigating in which reaction step water was present is challenging. Therefore, the assignment of reaction intermediates (Figure 2) and their chromatographic patterns directs to a facilitated identification of the error source. Consequently, a more stable radiotracer production is obtained.

2. Materials and Methods

Ethylmagnesium bromide (EtMgBr, 3.0 M in diethylether, in Sure-Seal™), thionyl chloride (SOCl₂) (99%), triethylamine (TEA; 99.5%), and tetrahydrofuran (THF, anhydrous, $\geq 99.9\%$, inhibitor-free) were purchased from Sigma-Aldrich (St. Louis, USA). Lithium aluminum hydride (LAH) (1.0 M in THF), (+)-PHNO standard, and precursor (+)-HNO hydrochloride (GMP and non-GMP) were obtained from ABX (Advanced Biochemical Compounds, Radeberg, Germany). All reagents were used without further purification. Sterile water and 0.9% saline solution were purchased from B. Braun (Melsungen, Germany). Sterile phosphate-buffered saline solution (0.021 M phosphate buffer, 0.188 M-NaCl, pH 7.7) was obtained from the Vienna General Hospital's Pharmacy (Vienna, Austria). The loop for the Grignard reactions is made of a 90 cm polyethylene (PE) tubing (fine bore polythene tubing REF 800/100/280; ID: 0.86 mm OD: 1.52 mm, Smiths Medical International Ltd.; Kent, UK). Ascarite II (20–30 mesh) was purchased from Thomas Scientific (Swedesboro, USA). Removal of acetonitrile was performed by using solid-phase extraction (SPE) cartridges (SepPak C18-plus) from Waters (Waters Cooperation; Milford, MA, USA). ^{11}C]CO₂ was produced by a GE PETtrace cyclotron 860 (General Electric Medical Systems; Uppsala, Sweden) via the $^{14}\text{N}(p,\alpha)^{11}\text{C}$ nuclear reaction by irradiation of a gas target (aluminum, irradiation parameters: 16 MeV protons, 10–25 mA) filled with high-purity N₂ (+1% O₂) (Air Liquide Austria GmbH, Schwechat, Austria). Automated syntheses were performed on a TRACERlab™ FX C Prosynthesizer (GE Healthcare, Uppsala, Sweden) including a semipreparative HPLC system featuring a Linear Instruments Model 200 UV/Vis detector and a LaPrep HPLC pump (VWR International GmbH; Vienna, Austria). For analytical HPLC, an Agilent 1260 infinity system (Agilent Technologies GmbH; Santa Clara, USA) incorporating a quaternary pump (G1311B), a column oven (G1316A), a manual injector (G1328C), a multi wavelength UV-detector (G1365D), and a NaI(Tl)-detector from Berthold Technologies (Bad Wildbad, Germany) was used. The HPLC device is controlled by GINA Star v5.9 SP17 controlling software (Elysia-Raytest; Straubenhardt, Germany).

2.1. Time Optimization on the Automated Synthesizer. A reduced reaction time was achieved by omitting all heating and cooling steps with exception of CO₂-trap heating. In particular, the target chamber was flushed twice with target gas prior to ^{11}C]CO₂ production and molecular sieves were preheated to 400°C for at least 15 min to minimize the content of nonradioactive ^{12}C]CO₂ within the target

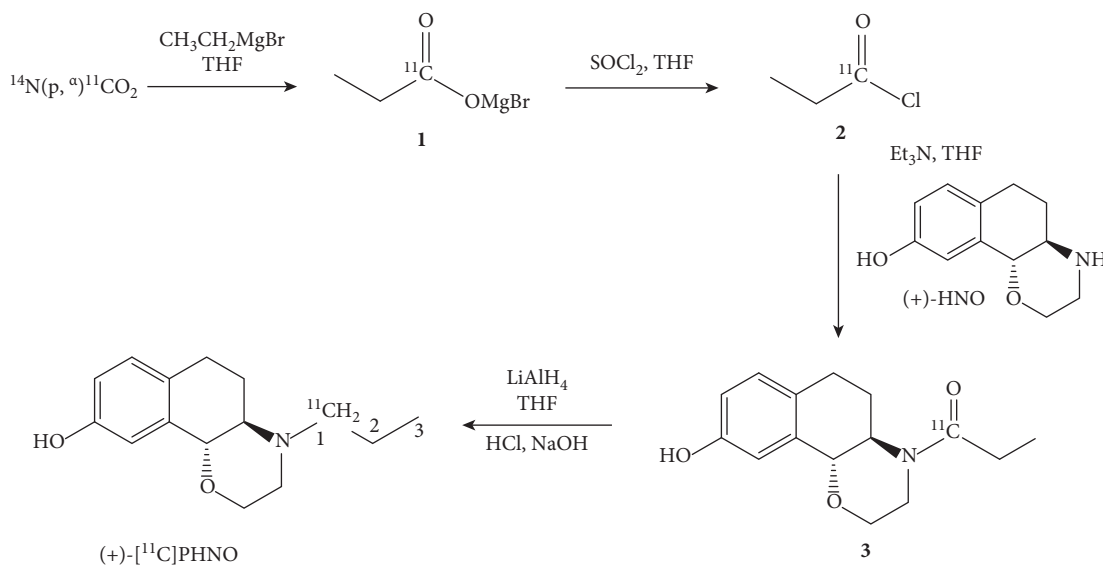


FIGURE 1: Synthesis scheme for the four-step radiosynthesis of (+)-[¹¹C]PHNO starting from cyclotron-produced [¹¹C]CO₂ and ethylmagnesium bromide.

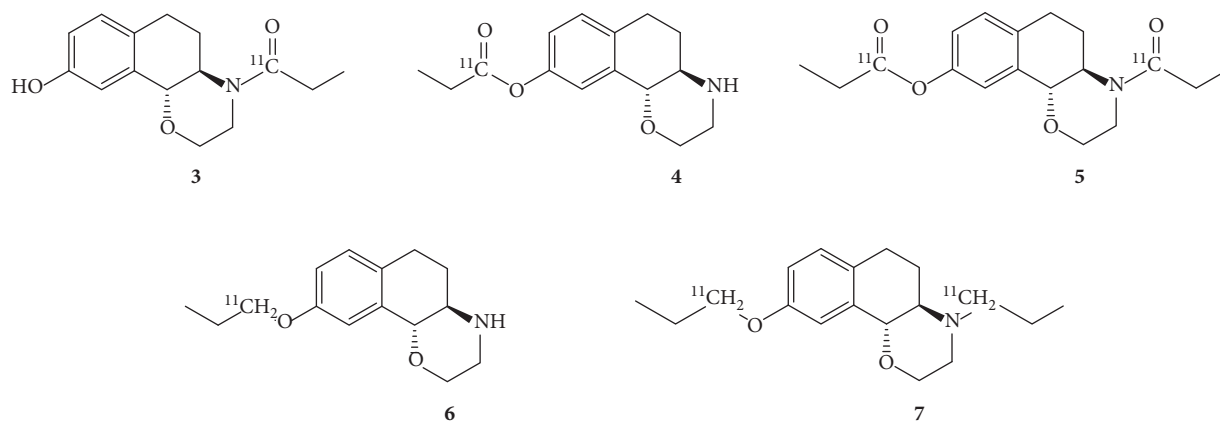


FIGURE 2: Chemical structure of the desired intermediate amide (compound 3) as well as nonreduced form of the side products (compounds 4 and 5) and reduced side products (compounds 6 and 7).

chamber and synthesizer. Afterwards, respective lines and tubings of the synthesizer were flushed with helium. After the production of the required amount of radioactivity, [¹¹C]CO₂ was released to the synthesizer and trapped on molecular sieve. Subsequently, the trapped [¹¹C]CO₂ was released by heating to 400°C under a He stream (5 mL/min) to a PE tube, which was beforehand impregnated with a solution of ethylmagnesium bromide (EtMgBr, 1 M) in THF. The impregnation was performed by diluting 500 μL EtMgBr with 1000 μL THF and pushing the solution through the loop, and then the loop was flushed with helium for around 5 sec to remove the excess of the impregnation solution. After the [¹¹C]CO₂ reaction with EtMgBr that last for around 5 min, SOCl₂ was pushed through the tube to obtain the acid chloride and the solution was simultaneously transferred to a reactor containing a solution of (+)-HNO (1.9–2.4 mg) in TEA (50 μL) and THF (400 μL). The intermediate amide species was obtained after 5–6 min stirring at room

temperature. Afterwards, a solution of 120 μL lithium aluminum hydride (LAH) in THF (400 μL) was added to reduce the intermediate amide. The reaction was quenched by addition of aqueous HCl (1 M, 900 μL) and neutralized with aqueous NaOH (1 M, 900 μL). The resulting suspension was filtered over cotton wool and purified by semipreparative HPLC. The collected product peak was diluted in 80 mL water and trapped on a C18-SPE cartridge. Afterwards, the product was eluted with 1.5 mL ethanol, diluted with phosphate buffered saline, and sterile filtered.

2.2. Evaluation of Temperatures for the Reduction Step with Lithium Aluminum Hydride (LAH). In order to evaluate the influence of the reaction temperature on the efficacy of the reduction of the intermediate amide with lithium aluminum hydride (LAH) to (+)-[¹¹C]PHNO, the synthesis was carried out using the following conditions:

- (i) -40°C (experimental set up as for -15°C)
- (ii) -15°C (as previously published by our group [21])
- (iii) 22°C (shortened synthesis time and no heating and cooling)

2.3. Partial Runs for the Investigation of Failed Syntheses.

Small-scale reactions and partial runs were conducted in borosilicate glass vials sealed with plastic septa as reaction vessel at room temperature. For all syntheses including the formation of the intermediate amide, a precursor solution of (+)-HNO (1–2 mg) in THF (400 μL) and TEA (50 μL) was used. The reaction was quenched by addition of H_2O (1 mL). For the identification of byproducts and investigation of the impact of individual reagents leading to failed synthesis, partial runs were performed as depicted in Figures 3 and 4.

- (1) Absence of TEA: the synthesis was conducted as described above, but without the use of triethylamine. The reaction was stopped either after the amide formation (A) or at the end of the whole production scheme (B).
- (2) Absence of SOCl_2 : the synthesis procedure was performed either without the addition of SOCl_2 (C) or in absence of both, SOCl_2 and LAH (D).
- (3) Absence of LAH: the synthesis was stopped before LAH addition to simulate a failed reduction of the amide (E).

2.4. Small-Scale Reactions and Partial Runs for the Analysis of an Insufficiently Inert Atmosphere. As Grignard reactions are especially sensitive to moisture, the impact of an insufficiently inert atmosphere and therefore contamination of the reagents with traces of water was investigated.

2.4.1. Influence of Moisture on the Grignard Reaction.

The effect of moisture before and after trapping of $[^{11}\text{C}]\text{CO}_2$ in EtMgBr was investigated as follows:

- (i) The PE tube was loaded with a mixture of 0.5 mL Grignard solution (3 M in Et_2O) in 1 mL THF, and then the activity was released through the loop. To quench the reaction and hydrolyse the radioactive intermediate, 0.5 mL of water was pushed through the impregnated loop and the reaction mixture was analyzed (F).
- (ii) 5 μL of water were added to the Grignard reagent solution and the reaction was stopped after amide formation (G) or after the reduction step (H).
- (iii) The PE tube was impregnated with the Grignard reagent solution and the loop was flushed with 0.5 mL of water. The reaction was stopped after amide formation (G1) or after the reduction step (H1).

2.4.2. Influence of Moisture on Acylation. The impact of moisture on the amide formation was investigated by adding

H_2O (20 μL) to a solution of (+)-HNO (1–2 mg) in THF (400 μL) and TEA (50 μL) prior to the addition of $[^{11}\text{C}]\text{propionic acid chloride}$ (I). Additionally, the same synthesis was performed and the resulting reaction mixture further treated with LAH (J).

2.5. Analytical and Semipreparative HPLC Measurements.

All crude, small-scale reaction mixtures were analyzed by analytical HPLC measurements as previously published by Nics et al. [22]. The stationary phase was an X-Bridge BEH Shield RP-18, 4.6×50 mm, 2.5 μm , 130 \AA column (Waters Cooperation; Milford, MA, USA). The mobile phase consisted of solvent A (ammonia phosphate buffer (100 mM), sodium-1-octasulfonate (5 mM), pH 2.1 adjusted with H_3PO_4); solvent B (90% acetonitrile (ACN)/10% water); solvent C (water); and solvent D (ammonium phosphate buffer (50 mM), pH 9.3 adjusted with NaOH). The gradient started with a composition of 33% A, 17% B, 17% C, and 33% D. Subsequently, B is increased over 2 min from 17% to 34%, whereas C is reduced from 17% to 0%. The UV/Vis signal was detected at a wavelength of 280 nm with a reference wavelength of 450 nm. The initial flow rate (1.5 mL/min) was decreased after 25 s to 1.0 mL/min. The retention time of the radioactive peaks was compared to the reference standard of (+)-PHNO in order to identify the respective product peak.

A part of the partial runs was additionally investigated on a semipreparative HPLC system with a Phenomenex Luna C18 column (250 \times 10 mm, 10 μm ; Phenomenex Ltd., Aschaffenburg, Germany) as a stationary phase. The mobile phase consisted of 25 mM phosphate-buffered saline (PBS) (pH 7.0)/ACN (60/40 v/v) with a flow rate of 5.8 mL/min. The UV/V is signal was measured at 254 nm. The peaks were collected and correlated with the respective peaks of the analytical HPLC.

2.6. Assignment of the Chromatographic Peaks of $[^{11}\text{C}]\text{CO}_2$ and $[^{nat}\text{C}]\text{Propionic Acid}$. $[^{11}\text{C}]\text{CO}_2$ was trapped in THF, and the solution was analyzed by analytical HPLC. The intermediate product propionic acid was injected to the analytical HPLC, and its retention time was compared to the radioactive impurity peaks of the crude mixture.

2.7. Synthesis of Compound 3 Using $[^{nat}\text{C}]\text{CO}_2$. The intermediate amide **3** was synthesized by using $[^{nat}\text{C}]\text{CO}_2$ gas that was bubbled through an EtMgBr solution (15 μL , 3.0 M in Et_2O) in THF (200 μL) for 3 min under He atmosphere. Afterwards, a solution of SOCl_2 (5 μL) in THF (400 μL) was added to generate the acyl chloride. After 4 min, the precursor solution of (+)-HNO (5 mg, non-GMP) in TEA (50 μL) and THF (200 μL) was added to the reaction mixture. The resulting suspension was extracted three times with CH_2Cl_2 (about 500 μL). The combined organic phases were injected into the semipreparative HPLC system. The collected peaks were analyzed by analytical HPLC and HRMS (ESI-MS: HNO ($\text{C}_{12}\text{H}_{16}\text{NO}_2$ [$\text{M} + \text{H}^+$] calcd. 206.118, found 206.118), **3** (or **4**) ($\text{C}_{15}\text{H}_{20}\text{NO}_3$ [$\text{M} + \text{H}^+$] calcd. 262.144, found 262.143, $\text{C}_{15}\text{H}_{19}\text{NO}_3\text{Na}$ [$\text{M} + \text{Na}^+$] calcd. 284.126,

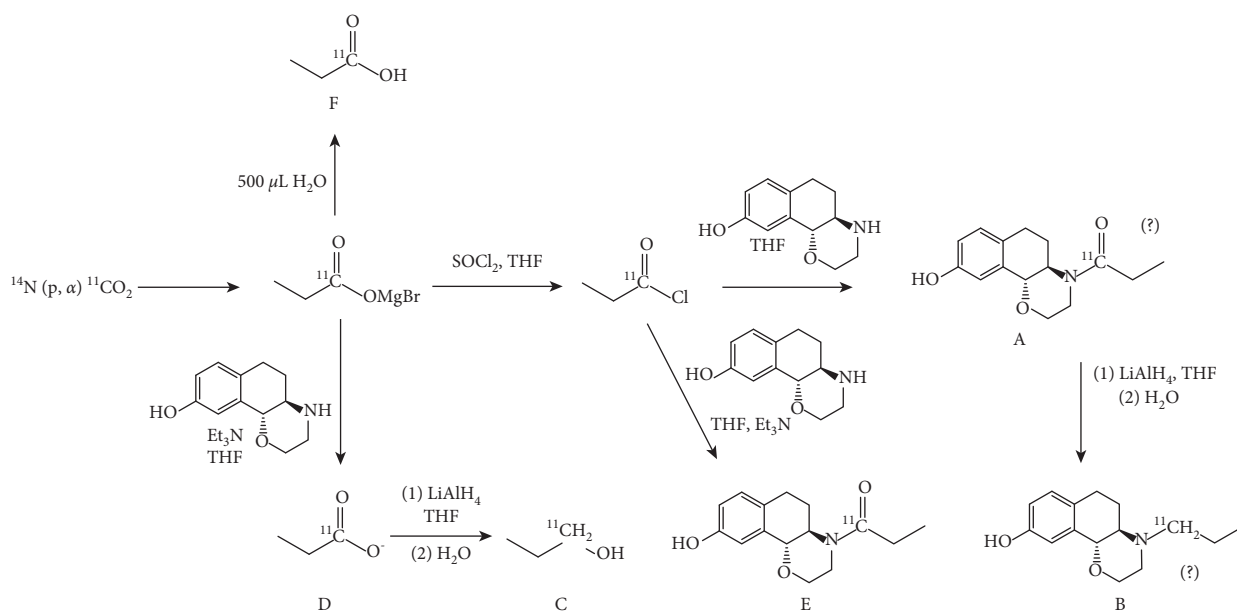


FIGURE 3: Reaction scheme of partial runs A-E for investigation of reaction intermediates formed during (+)-[^{11}C]PHNO radiosynthesis.

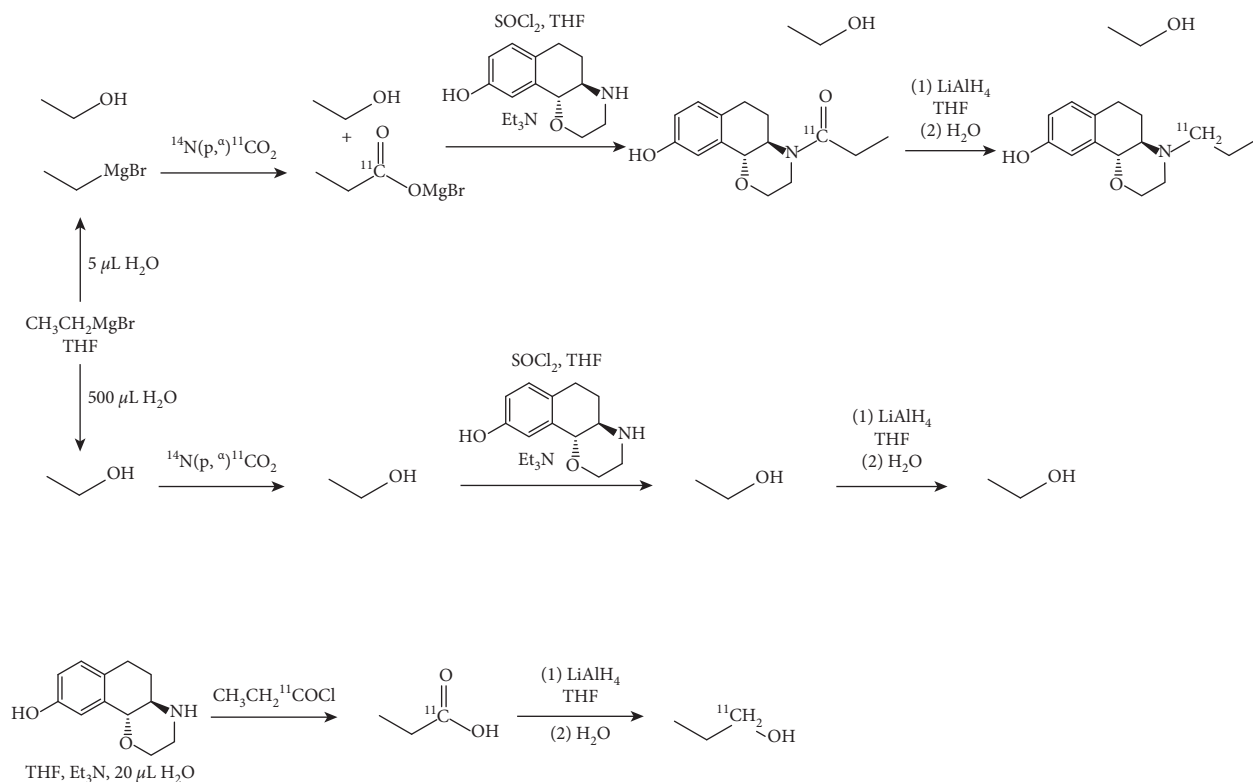


FIGURE 4: Reaction scheme of partial runs G-J for investigation of reaction intermediates formed during (+)-[^{11}C]PHNO radiosynthesis.

found 284.125), and **5** ($\text{C}_{18}\text{H}_{24}\text{NO}_4$ [$\text{M} + \text{H}^+$] calcd. 318.171, found 318.170, $\text{C}_{18}\text{H}_{23}\text{NO}_4\text{Na}$ [$\text{M} + \text{Na}^+$] calcd. 340.153, found 340.152).

2.8. Characterization of Intermediate Compounds and Side Products. Characterization and identification of the compounds separated by HPLC was performed by high-

resolution mass spectrometry (HRMS) on a Bruker maXis UHR-TOF device (electrospray ionization (ESI); qQ-TOF, mass accuracy < 5 ppm) in either positive or negative mode depending on the respective molecular structure.

2.9. Definition of Yield Determination. According to the consensus of nomenclature, the activity yield is defined as

the amount of product that is obtained after a synthesis in MBq or GBq and is not corrected for decay. This term is related to the starting activity of $[^{11}\text{C}]\text{CO}_2$ and can be expressed in [%] as radiochemical yield not corrected for decay [23].

2.10. Statistical Analysis. Study data were obtained from all syntheses performed in our department between 01/2017 and 08/2017 with starting activity of 100–150 GBq at the end of bombardment (EOB) of $[^{11}\text{C}]\text{CO}_2$. Values are given as mean values \pm SD as calculated with Microsoft Excel 2010 if not stated otherwise. Statistical analysis was performed by using a *t* test as implemented in Graph Pad Prism 6 (GraphPad Software, La Jolla, USA).

3. Results and Discussion

3.1. Reduction of the Radiosynthesis Duration for an Improved Activity Yield. The previously described radiosynthetic process for (+)- $[^{11}\text{C}]\text{PHNO}$ preparation by Rami-Mark et al. involves a heating step to 80°C for the acylation reaction, followed by the addition of LAH at –15°C [21]. Afterwards, the residual THF is removed via distillation (Figure 5).

In the improved method, all reaction steps of (+)- $[^{11}\text{C}]\text{PHNO}$ synthesis were performed at room temperature. In detail, the acylation with $[^{11}\text{C}]\text{propionic acid chloride}$ was performed without heating and cooling as well as the addition of LAH. In this study, the improved synthesis ($n = 16$) was compared with two experimental setups: (1) (+)- $[^{11}\text{C}]\text{PHNO}$ synthesis was conducted as previously described by our group ($n = 9$) [19]. (2) LAH was added at –40°C as described by Wilson et al. ($n = 3$) [12]. Performing all reaction steps at room temperature realized an average reduction of the overall synthesis time by around 5 min (approximately 13% in comparison to the previously published synthesis [21]) as described in Figure 6. This time reduction is especially beneficial for the production of a ^{11}C -radiotracer as it impedes loss of radiolabeled product by decay of around 15%. As a result, the activity yield was increased in comparison to previously published synthetic procedures. Synthesis at room temperature led to a significantly increased isolated radiochemical yield not corrected for decay of $1.4 \pm 0.8\%$. All yields within this manuscript were calculated by referring the product activity to the activity after the end of bombardment. [23] Indeed, the experiments in which the reduction was carried out at –15 or –40°C resulted in $0.53 \pm 0.17\%$ and $0.50 \pm 0.11\%$ isolated radiochemical yield without decay correction, respectively (Figure 6). Thus, this study clearly showed that (+)- $[^{11}\text{C}]\text{PHNO}$ synthesis can be successfully performed at room temperature without a forfeit of activity yield. The starting activities and activity yields of the experiments are given in Table 1.

The success rate of the synthesis at room temperature exceeds the success rate of our previously published method by Rami-Mark et al. (Table 1) [21]. The success rate of LAH addition at –40°C is 100%, but it should be considered that the number of performed experiments is only 3.

The limiting parameter of the reaction at room temperature is the reactor volume as the solvent is not evaporated and an overflow of the reaction mixture must be avoided. If an adequate reactor is available, this facilitated four-step synthesis procedure can be performed in every radiochemistry laboratory that is equipped with a cyclotron. All experiments showed a similar pattern of the crude reaction mixture in semipreparative as well as analytical HPLC chromatograms but a different intensity of the peaks (Figure 7). The peaks with a retention time of 0–26 s are hydrophilic compounds like $[^{11}\text{C}]\text{CO}_2$ and $[^{11}\text{C}]\text{propionic acid}$. The species at 47 s and 48 s are probably the carbonyl intermediates. The peak at a retention time range of 1 min 55 sec to 2 min 10 sec originate from (+)- $[^{11}\text{C}]\text{PHNO}$. However, after purification by semipreparative HPLC, (+)- $[^{11}\text{C}]\text{PHNO}$ could be obtained in an excellent purity of >95% for all applied methods.

3.2. Partial Runs for the Investigation of Failed Synthesis. Radioactive reaction intermediates and byproducts were found at retention times of 2–3 min, 3–4 min, 4.8 min, 6 min, and 8 min within semipreparative HPLC, as well as of 20 s, 45 s, and 2.5 min in analytical HPLC, respectively, for successful (+)- $[^{11}\text{C}]\text{PHNO}$ synthesis (Figures 7(a) and 8(a)). Partial runs of the synthesis were performed to identify the byproducts and therefore the respective error sources.

3.2.1. Absence of Triethylamine. The syntheses were performed in absence of triethylamine, and therefore, the precursor (+)-HNO was still protonated. Syntheses were either stopped at the intermediate amide (route A) or conducted until the end of synthesis (route B).

In route A, semipreparative HPLC showed the main species at a retention time of 2.5–3 min (Figure 8(b)), and in analytical HPLC, the main peak was observed at short retention times (15–20 s and comprised about $66.8 \pm 0.2\%$), usually representing small hydrophilic compounds, like $[^{11}\text{C}]\text{CO}_2$ and $[^{11}\text{C}]\text{propionic acid}$. Further peaks with smaller intensities were observed at longer retention times (4.5 min and 6 min in semipreparative HPLC) showing minor amounts of potential carbonyl byproducts (compound 3 or 4) resulting from an insufficient deprotonation of the precursor, which impedes the acylation process.

Reaction scheme B, which included the reduction step with LAH, shows similar chromatographic pattern. However, no product formation was observed showing that deprotonation of (+)-HNO is pivotal for a successful (+)- $[^{11}\text{C}]\text{PHNO}$ synthesis. In conclusion, a chromatogram with intensive signals at early retention times, poor signal at retention times of 5–6.5 min, and no formation of product may originate from nonintact Et_3N .

3.2.2. Absence of SOCl_2 . All experiments, which were performed without SOCl_2 , were either stopped after theoretical amide formation (C) or after the reduction step (D). Semipreparative HPLC showed only peaks with retention time <4 min and no product formation. A similar picture

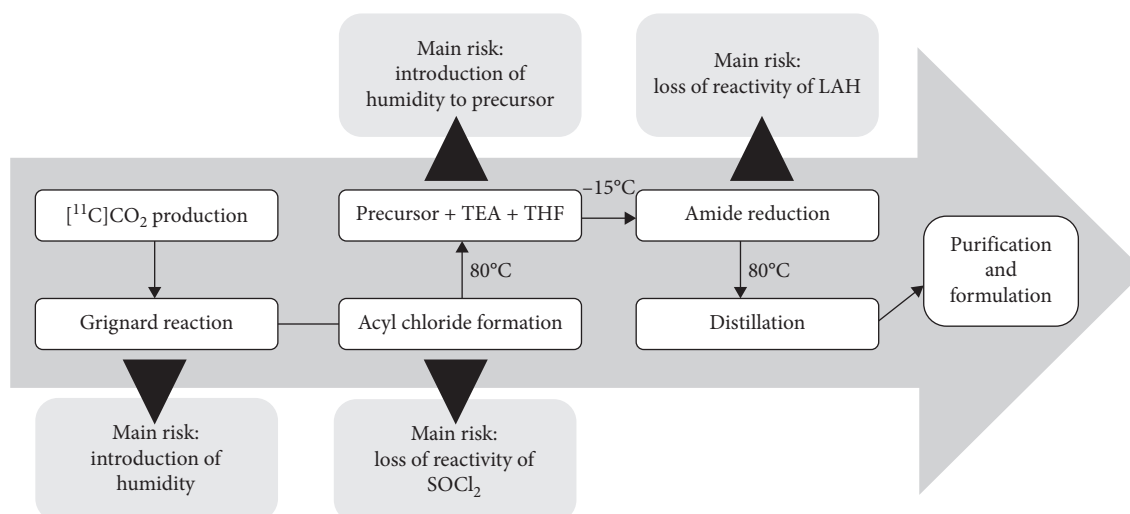


FIGURE 5: Reaction steps of (+)- ^{11}C]PHNO production according to Rami-Mark et al. [21] with the corresponding main risk for each reaction step.

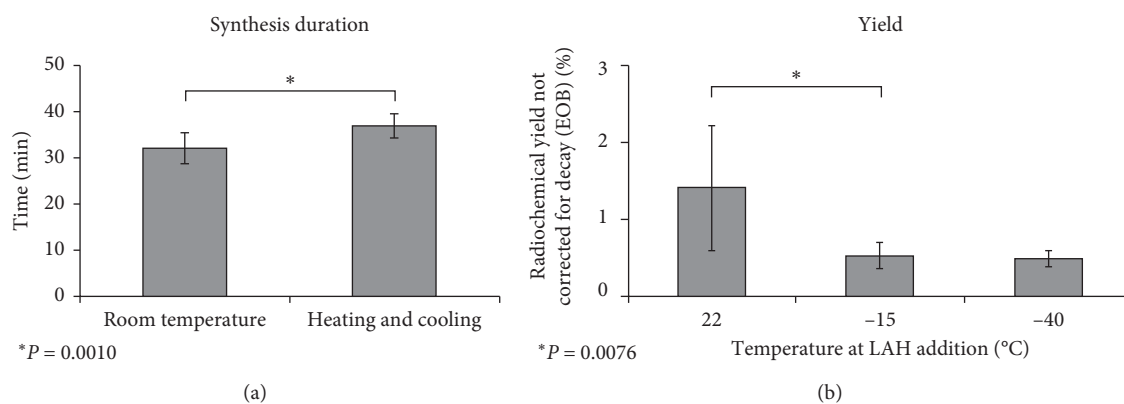


FIGURE 6: (a) Comparison of the synthesis duration of (+)- ^{11}C]PHNO synthesis at room temperature ($n = 16$) and according to our previously published method including heating and cooling ($n = 9$). (b) Influence of the temperature at LAH addition on the isolated radiochemical yield not corrected for decay (22 $^{\circ}\text{C}$: $n = 16$, -15 $^{\circ}\text{C}$: $n = 9$, -40 $^{\circ}\text{C}$: $n = 3$).

TABLE 1: Starting activity, activity yield, number of experiments, and success rate of the studied experimental setups.

Temperature at LAH addition ($^{\circ}\text{C}$)	Starting activity (EOB) (GBq)	Activity yield (GBq)	n	Success rate (%)
22	120 \pm 15	1.7 \pm 1.0	16	89
-15	122 \pm 13	0.7 \pm 0.2	9	82
-40	113 \pm 8	0.6 \pm 0.1	3	100

was observed for analytical HPLC. Thus, complete absence of high retention-time peaks indicates inactivated or decomposed SOCl_2 .

3.2.3. Absence of LAH. Simulation of a failed LAH-reduction step was done by stopping prior to the reduction step (E). Here, a radioactive peak at a retention time of 6 min could be observed in semipreparative HPLC. This peak also occurred in other experiments without LAH (route B) and therefore potentially represents a carbonyl species, namely, **3**, **4**, or **5**. Furthermore, the signal could be assigned to the 45 s peak in analytical HPLC being the

most prominent one with an intensity of 51 \pm 22%. A highly dominant peak in the semipreparative HPLC chromatogram at 6 min without product formation conclusively points to a failed LAH-reduction. As a consequence, a new bottle of LAH should be used for following syntheses and special attention should be paid to the inert atmosphere.

3.3. Small-Scale Reactions and Partial Runs for the Analysis of an Completely Inert Atmosphere. For investigating the influence of minor amounts of moisture on the Grignard reagent, following experiments were performed:

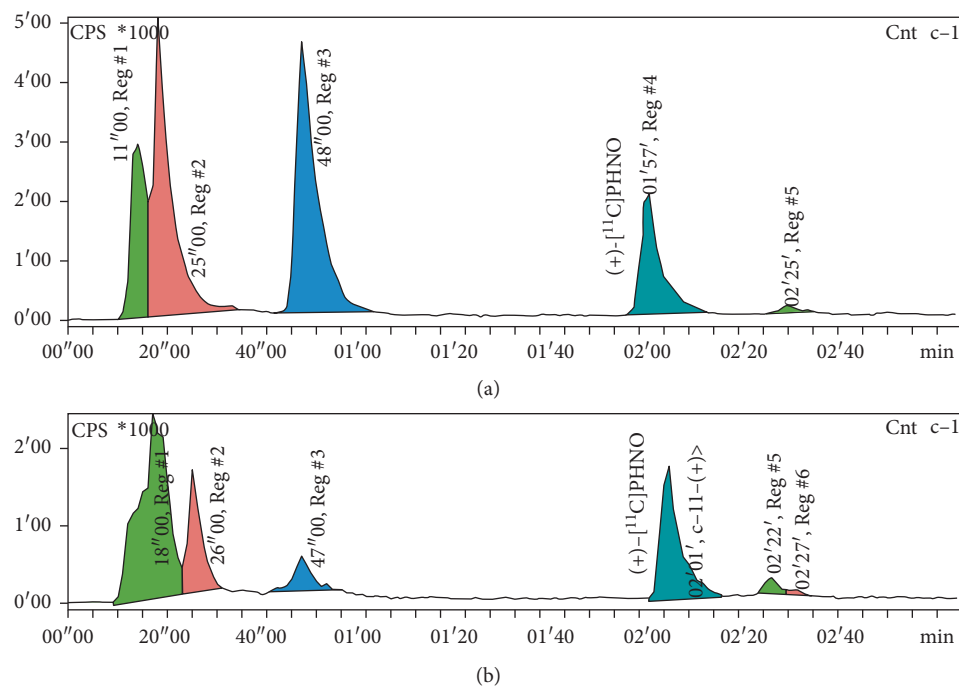


FIGURE 7: Analytical HPLC chromatograms of the crude reaction mixtures obtained by addition of LAH at room temperature (a) or at -40°C (b).

- (i) Hydrolysis of the Grignard reagent after the addition of $[^{11}\text{C}]\text{CO}_2$ (route F)
- (ii) Adding water to the Grignard reagent before addition of $[^{11}\text{C}]\text{CO}_2$ (routes G and H)

In addition, the moisture sensitivity of the acylation was tested by intentionally adding water to the precursor solution (routes I and J).

3.3.1. Influence of Moisture on the Grignard Reaction.

The route F led to semipreparative chromatographic peaks at retention times of 2–3 min, 3–5 min, and 6.0–6.5 min. In this respect, analytical HPLC displayed a main signal at a retention time of 15–20 s ($75 \pm 7\%$). Surprisingly, we also observed peaks at 45 s and 2.5 min, although the expected species, propionic acid and $[^{11}\text{C}]\text{CO}_2$, are supposed to elute at earlier retention times.

Simulation of a Grignard reaction under an insufficiently inert atmosphere on the acylation was performed by directly adding $5\ \mu\text{L}$ water to the Grignard reagent (G and G1), whereas for a complete quenching of the reaction, $500\ \mu\text{L}$ water was added (H and H1).

When the reaction process was stopped after amide formation, an intensive peak at 6 min was visible in semipreparative HPLC for an addition of $5\ \mu\text{L}$, whereas this peak was not detected for $500\ \mu\text{L}$. Hence, the occurrence of this peak shows that $5\ \mu\text{L}$ water is not sufficient for quenching the Grignard reaction completely due to stoichiometric reasons: 15 mmol of EtMgBr are used for the reaction and $0.28\ \text{mmol H}_2\text{O}$ was added. Therefore, as a relatively huge amount of water is needed for a fail in synthesis, moisture alone will not lead to a quenched reaction. This effect could

be confirmed by conducting the complete reaction process. Addition of $5\ \mu\text{L}$ water to the Grignard solution (route H) leads to minor amounts of $(+)\text{-}[^{11}\text{C}]\text{PHNO}$, whereas the addition of $500\ \mu\text{L}$ of water (H1) completely quenched all further reactions. As a consequence, the presence of peaks with a retention time less than 4 min in semipreparative HPLC may originate from a decomposed Grignard reagent.

Besides, the peaks of the semipreparative HPLC and analytical HPLC were correlated to each other as follows (Figure 9): retention times below 3 min (semipreparative HPLC) corresponds to a peak at 20 s (analytical HPLC), the peaks between 3 min and 5 min 30 s are similar to the one at 2 min 30 s, and the 6 min peak to the one at 45 s. Accordingly, the two peaks of 3–5 min 30 s and 6 min in semipreparative HPLC switched their retention order in the analytical run.

3.3.2. Influence of Moisture on Acylation.

Here, $20\ \mu\text{L}$ water was added to the precursor solution ($400\ \mu\text{L}$ THF, $50\ \mu\text{L}$ TEA, $0.9\text{--}1.4\ \text{mg (+)-HNO}$) prior to addition of intact propionic acid chloride. The synthesis was stopped after formation of the amide (I) or after the reduction (J). For partial run I, the ratio of the reaction intermediates was as follows: 15–20 s and 45 s with 37.5% and 34.0%, respectively. Due to the high intensity of the peak at 45 s, it can be assumed that the reaction was not completely quenched and one of the carbonyl species was partly formed. Likewise, semipreparative HPLC revealed signals at 4–7 min indicating carbonyl formation. Performing the entire synthetic route for $(+)\text{-}[^{11}\text{C}]\text{PHNO}$ production (J) leads to a peak at a retention time similar to $(+)\text{-}[^{11}\text{C}]\text{PHNO}$ (9 min) with low intensity. However, analytical HPLC showed a peak at 1 min

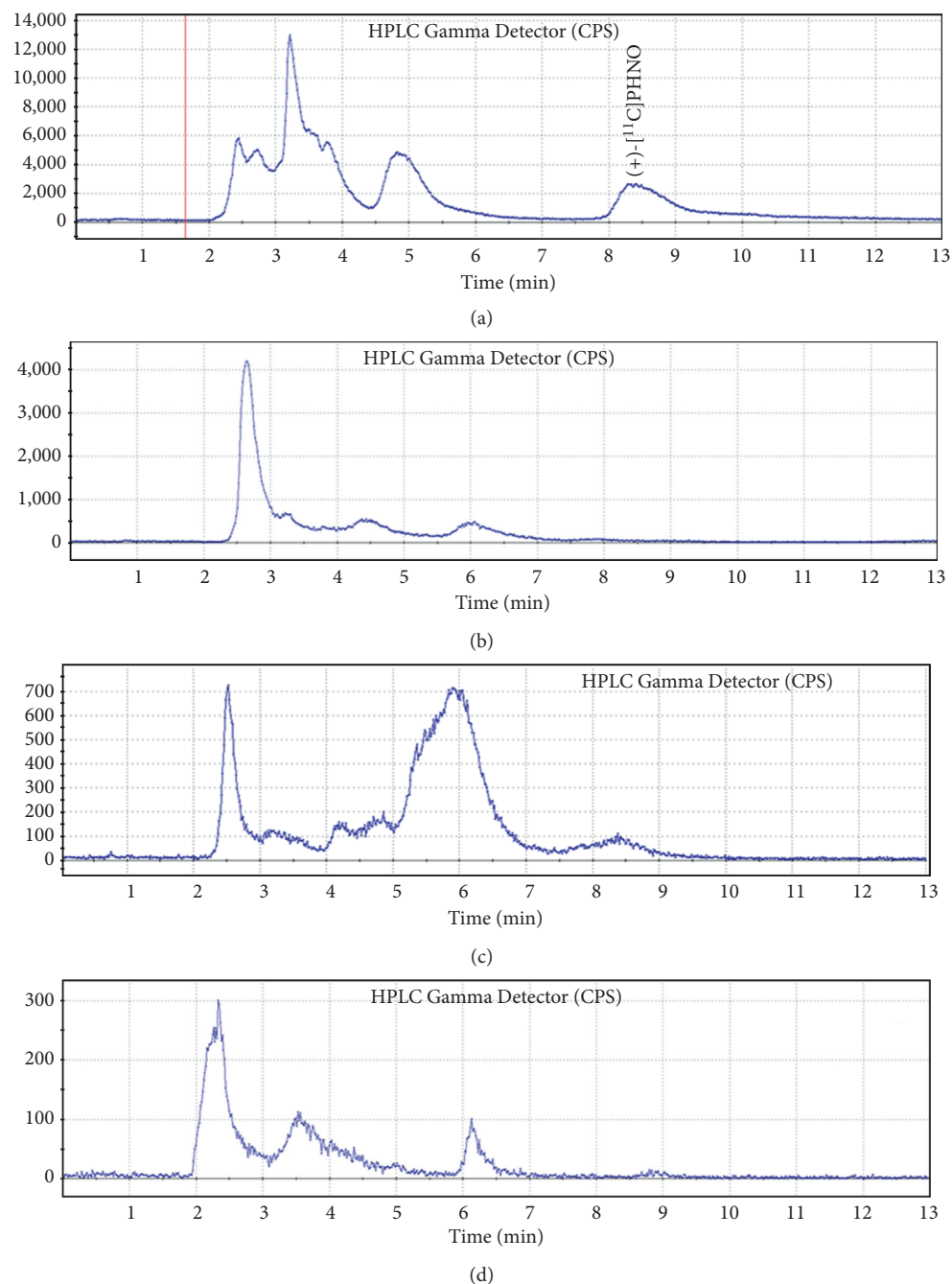


FIGURE 8: Chromatogram of semipreparative HPLC of full synthesis at room temperature (a), route A synthesis without TEA and LAH (b), route E without LAH (c), and route F in which the reaction is quenched after Grignard reaction (d).

26 s with 8.3% conversion but no signal at 2 min for the product. This chromatographic pattern is quite similar to the one observed for the partial run without TEA.

3.4. Assignment of the Chromatographic Peaks of $[^{nat}C]$ Propionic Acid and $[^{11}C]CO_2$. One intermediate of (+)- $[^{11}C]$ PHNO synthesis is $[^{11}C]$ propionic acid, which was identified by comparison of the nonradioactive reference compound $[^{nat}C]$ propionic acid. The analytical chromatogram showed a

signal at 15–40 s at 280 nm wavelength (Figure 10). Moreover, $[^{11}C]CO_2$ was trapped in THF to assign the respective peak as well. The signal was found at a retention time of 20–40 s similar to $[^{nat}C]$ propionic acid (Figure 10). Hence, both compounds, $[^{11}C]CO_2$ as well as $[^{11}C]$ propionic acid, are not base line separated and were present in nearly every analytical chromatogram. Those results support the previously obtained data, showing that the exclusive presence of early eluting peaks indicates problems within the first reaction steps preventing amide formation.

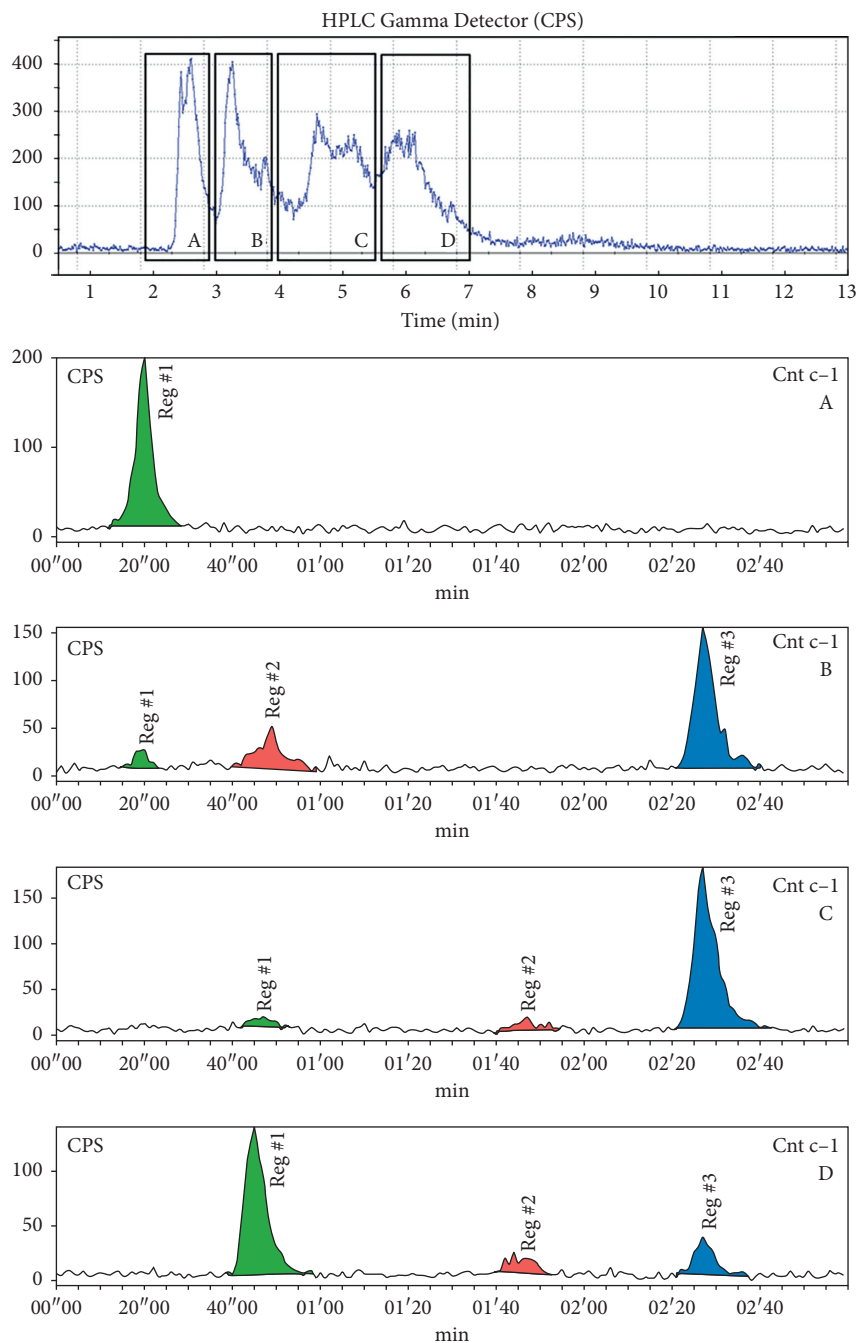


FIGURE 9: Semipreparative HPLC chromatogram of partial run G and the corresponding analytical chromatograms of the respective peak.

3.5. Synthesis of Compound 3 Using $[^{nat}C]CO_2$ for Assignment of HPLC Peaks. The cold synthesis of the intermediate amide resulted in a crude reaction mixture that was transferred onto semipreparative HPLC. The fractions were collected and measured by HRMS (high-resolution mass spectrometry). The respective signal of the precursor, as well as of compounds 3 or 4 and 5 could be identified (see Materials). As 3 and 4 have the same molecular weight, those two molecules cannot be differentiated by mass spectrometry. Besides, the formation of byproducts 5 and 7 during radiosynthesis is very unlikely due to substoichiometric ratio in radiosynthesis.

3.6. Establishment of a Troubleshooting Protocol. As shown in this study, failure of (+)- $[^{11}C]PHNO$ radiosynthesis can be attributed to various reasons, but the chromatogram of the semipreparative HPLC provides information on error sources. Based on our results, we created a decision scheme that helps troubleshooting in case of a failed (+)- $[^{11}C]PHNO$ production (Figure 11). The presence of intensive and broad peaks in the region of 5–7 min shows a successful carbonylation but a failed reduction to (+)- $[^{11}C]PHNO$. Consequently, the LAH should be renewed. If there is at least one broad peak with low intensity in this range, the amide formation was incomplete, which is mainly attributed to

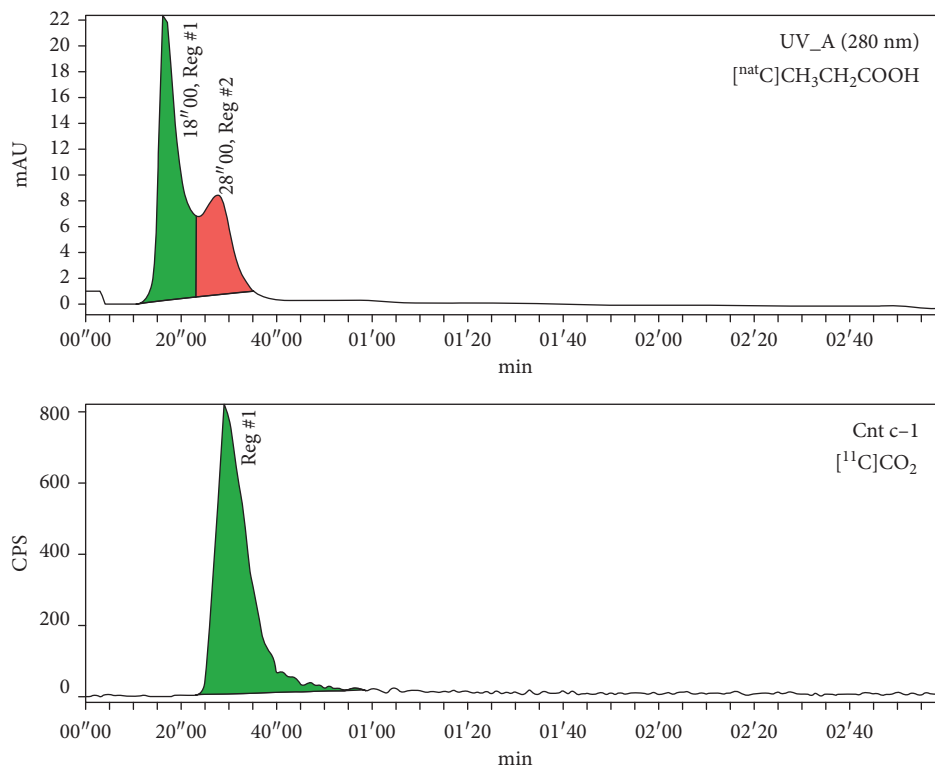


FIGURE 10: (a) UV/Vis chromatogram of $[^{nat}\text{C}]\text{propionic acid}$. (b) Radio-channel chromatogram of $[^{11}\text{C}]\text{CO}_2$.

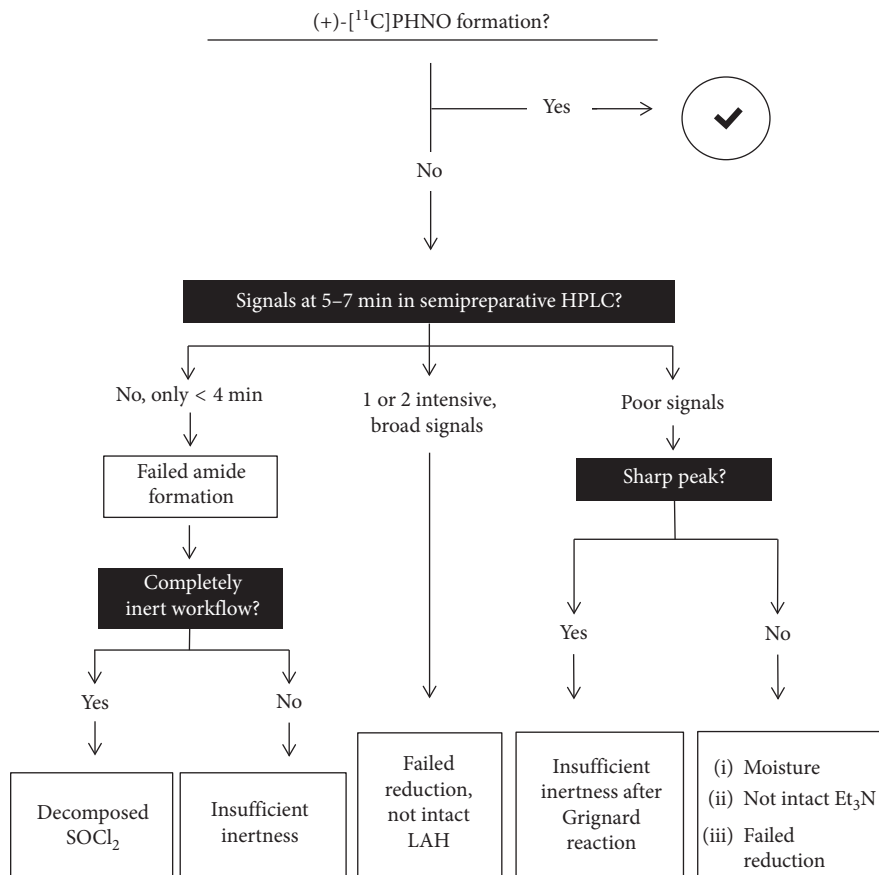


FIGURE 11: Schematic decision tree aiding troubleshooting after a failed (+)- $[^{11}\text{C}]\text{PHNO}$ formation.

moisture. In addition, a single, sharp peak between 5 and 7 min suggests the presence of water after the Grignard reaction. A chromatogram that is missing those signals indicates a failure in the coupling and can be assigned to a poor inert atmosphere or decomposed SOCl_2 . Hence, the SOCl_2 should be changed. This scheme will facilitate troubleshooting and lead to an improved rate of successful (+)-[^{11}C]PHNO.

4. Conclusion

The complex synthesis of (+)-[^{11}C]PHNO is a challenge for every radiochemist in terms of time efficiency, reduction of failed syntheses, and error evaluation. Here, we present a new method allowing a tremendous reduction of the radiosynthetic duration of approximately 5 min by omitting heating and cooling steps, which enhances the activity yield significantly. Moreover, the investigation of side products and intermediate species facilitates the error evaluation after a failed synthesis. Accordingly, we propose a decision tree to support troubleshooting and facilitating a stable and continuous radiotracer production that is a necessity for clinical studies.

Data Availability

The synthesis and the preparative HPLC data used to support the findings of this study are available from the corresponding author upon request. The quality control data used to support the findings of this study are included within the article.

Conflicts of Interest

The authors declare that there are no conflicts of interest.

Acknowledgments

We thank Thomas Zenz and Andreas Krcal for technical support and their “around the clock” availability. Moreover, Thomas Kalina, Chrysoula Vraka, Jens Cardinale, Marie Brandt, and Marius Ozenil are thanked for scientific discussions and support. This work was supported by the the Vienna Science and Technology Fund (WWTF; grant No. CS15-033) granted to Matthäus Willeit.

References

- [1] P. Seeman, C. Ulpian, R. D. Larsen, and P. S. Anderson, “Dopamine receptors labelled by PHNO,” *Synapse*, vol. 14, no. 4, pp. 254–262, 1993.
- [2] A. Breier, T. P. Su, R. Saunders et al., “Schizophrenia is associated with elevated amphetamine-induced synaptic dopamine concentrations: evidence from a novel positron emission tomography method,” *Proceedings of the National Academy of Sciences*, vol. 94, no. 6, pp. 2569–2574, 1997.
- [3] S. Hisahara and S. Shimohama, “Toxin-Induced and Genetic animal models of Parkinson’s disease,” *Parkinson’s Disease*, vol. 2011, pp. 1–14, 2011.
- [4] A. Graff-Guerrero, M. Willeit, N. Ginovart et al., “Brain region binding of the D2/3 agonist [^{11}C]-(+)-PHNO and the D2/3 antagonist [^{11}C]raclopride in healthy humans,” *Human Brain Mapping*, vol. 29, no. 4, pp. 400–410, 2008.
- [5] J.-D. Gallezot, J. D. Beaver, R. N. Gunn et al., “Affinity and selectivity of [^{11}C]-(+)-PHNO for the D3 and D2 receptors in the rhesus monkey brain in vivo,” *Synapse*, vol. 66, no. 6, pp. 489–500, 2012.
- [6] M. Willeit, N. Ginovart, A. Graff et al., “First human evidence of d-amphetamine induced displacement of a D2/3 agonist radioligand: a [^{11}C]-(+)-PHNO positron emission tomography study,” *Neuropsychopharmacology*, vol. 33, no. 2, pp. 279–289, 2008.
- [7] N. Ginovart, L. Galineau, M. Willeit et al., “Binding characteristics and sensitivity to endogenous dopamine of [^{11}C]-(+)-PHNO, a new agonist radiotracer for imaging the high-affinity state of D2 receptors in vivo using positron emission tomography,” *Journal of Neurochemistry*, vol. 97, no. 4, pp. 1089–1103, 2006.
- [8] R. Mizrahi, J. Addington, P. M. Rusjan et al., “Increased stress-induced dopamine release in psychosis,” *Biological Psychiatry*, vol. 71, no. 6, pp. 561–567, 2012.
- [9] H.-H. Tseng, J. J. Watts, M. Kiang et al., “Nigral stress-induced dopamine release in clinical high risk and antipsychotic-naïve schizophrenia,” *Schizophrenia Bulletin*, vol. 44, no. 3, pp. 542–551, 2018.
- [10] S. M. Ametamey, M. Honer, and P. A. Schubiger, “Molecular imaging with PET,” *Chemical Reviews*, vol. 108, no. 5, pp. 1501–1516, 2008.
- [11] M. Willeit, N. Ginovart, S. Kapur et al., “High-affinity states of human brain dopamine D2/3 receptors imaged by the agonist [^{11}C]-(+)-PHNO,” *Biological Psychiatry*, vol. 59, no. 5, pp. 389–394, 2006.
- [12] A. A. Wilson, P. McCormick, S. Kapur et al., “Radiosynthesis and evaluation of [^{11}C]-(+)-4-Propyl-3,4,4a,5,6,10b-hexahydro-2H-naphtho[1,2-b][1,4]oxazin-9-ol as a potential radiotracer for in vivo imaging of the dopamine D2 high-affinity state with positron emission tomography,” *Journal of Medicinal Chemistry*, vol. 48, no. 12, pp. 4153–4160, 2005.
- [13] C. Plisson, M. Huiban, S. Pampols-Maso, G. Singleton, S. P. Hill, and J. Passchier, “Automated preparation of the dopamine D2/3 receptor agonist ligand [^{11}C]-(+)-PHNO for human PET imaging studies,” *Applied Radiation and Isotopes*, vol. 70, no. 2, pp. 380–387, 2012.
- [14] S. Oya, S. K. Joseph, P. Carberry, C. R. Divgi, and A. O. Koren, “Preparation of [^{11}C]-(+)-PHNO using an automated synthesizer coupled with a stand-alone system for making [^{11}C] propionyl chloride,” *Journal of Labelled Compounds and Radiopharmaceuticals*, vol. 466, 2013.
- [15] D. E. Payer, M. Guttman, S. J. Kish et al., “D₃ dopamine receptor-preferring [^{11}C]PHNO PET imaging in Parkinson patients with dyskinesia,” *Neurology*, vol. 86, pp. 224–230, 2016.
- [16] E. C. Gaiser, J.-D. Gallezot, P. D. Worhunsky et al., “Elevated dopamine D2/3 receptor availability in obese individuals: a PET imaging study with [^{11}C](+)PHNO,” *Neuropsychopharmacology*, vol. 41, no. 13, pp. 3042–3050, 2016.
- [17] S. Malik, M. Jacobs, S.-S. Cho et al., “Deep TMS of the insula using the H-coil modulates dopamine release: a crossover [^{11}C] PHNO-PET pilot trial in healthy humans,” *Brain Imaging and Behavior*, vol. 12, no. 5, pp. 1306–1317, 2018.
- [18] D. W. McPherson, D.-R. Hwang, J. S. Fowler, A. P. Wolf, R. M. Macgregor, and C. D. Arnett, “A simple one-pot synthesis of cyclopropane [^{11}C]carbonyl chloride. Synthesis and biodistribution of [^{11}C]cyclophphan,” *Journal of Labelled*

- Compounds and Radiopharmaceuticals*, vol. 23, no. 5, pp. 505–514, 1986.
- [19] S. K. Luthra, D. Le Bars, V. W. Pike, and F. Brady, “Preparation of NCA [^{11}C]acid chlorides as labelling agents for amides,” *Journal of Labelled Compounds and Radiopharmaceuticals*, vol. 26, no. 1-12, pp. 66–68, 1989.
- [20] S. K. Luthra, V. W. Pike, and F. Brady, “Preparation of some NCA [^{11}C]acid chlorides as labelling agents,” *International Journal of Radiation Applications and Instrumentation. Part A. Applied Radiation and Isotopes*, vol. 41, no. 5, pp. 471–476, 1990.
- [21] C. Rami-Mark, J. Ungersboeck, D. Haeusler et al., “Reliable set-up for in-loop ^{11}C -carboxylations using Grignard reactions for the preparation of [carbonyl- ^{11}C]WAY-100635 and [^{11}C]-(+)-PHNO,” *Applied Radiation and Isotopes*, vol. 82, pp. 75–80, 2013.
- [22] L. Nics, B. Steiner, E.-M. Klebermass et al., “Speed matters to raise molar radioactivity: fast HPLC shortens the quality control of C-11 PET-tracers,” *Nuclear Medicine and Biology*, vol. 57, pp. 28–33, 2018.
- [23] H. H. Coenen, A. D. Gee, M. Adam et al., “Consensus nomenclature rules for radiopharmaceutical chemistry—setting the record straight,” *Nuclear Medicine and Biology*, vol. 55, pp. v–xi, 2017.